Journal of Alloys and Compounds 855 (2021) 157435

Contents lists available at ScienceDirect

Journal of Alloys and Compounds

journal homepage: http://www.elsevier.com/locate/jalcom

Structural and magnetic properties of new members of the 3:29 phase from the Ce–Fe–Mn system and 1:11 from the Ce–Co–Mn

Vitalii Shtender [a], Daniel Hedlund [b], Simon Rosenqvist Larsen [a], Peter Svedlindh [b], Martin Sahlberg [a, *]

[a] Department of Chemistry – Ångström Laboratory, Uppsala University, Box 538, 75121, Uppsala, Sweden
[b] Solid State Physics, Department of Materials Science and Engineering, Uppsala University, Sweden

ARTICLE INFO

Article history:
Received 16 June 2020
Received in revised form
8 September 2020
Accepted 1 October 2020
Available online 2 October 2020

Keywords:
Intermetallic compounds
Crystal structure
Magnetic properties

ABSTRACT

The Ce–Fe–Mn and Ce–Co–Mn systems have been re-visited with the intent of finding new potential phases for application as permanent magnets. Two new ternary compounds, $Ce_3(Fe_{0.638}Mn_{0.362})_{29}$ ($Nd_3(Fe,Ti)_{29}$-type, space group $P2_1/c$, No. 14, Pearson Symbol $mP128$) and $CeCo_8Mn_3$ ($Ce(Ni,Mn)_{11}$-type, space group $P4/mbm$, No. 127, Pearson Symbol $tP24$) have been discovered in the compositional range where the $Ce_2(T,Mn)_{17}$ (T = Fe, Co) phases are expected to exist with a (H)–Th_2Ni_{17}-type structure (space group $P6_3/mmc$, No. 194, Pearson Symbol $hP38$). Detailed investigations of the crystal structures have been performed using X-ray powder diffraction (XRPD) with supporting energy-dispersive X-ray (EDS) analysis. Compositions of the new compounds have been defined based on the EDS analysis as follows: $Ce_{9.7}Fe_{57.5}Mn_{32.8}$ and $Ce_{9.2}Co_{65.2}Mn_{25.6}$. A short discussion on the crystal structure peculiarities of the 1:5, 1:11, 1:12, 2:17 and 3:29 compounds in the Ce–T–Mn (T = Fe, Co, Ni, Cu) systems has been made. We present magnetic measurements on selected representatives of the studied phases. The most interesting being the $Ce_3(Fe_{0.638}Mn_{0.362})_{29}$ phase which has a transition temperature well above room temperature. $CeNi_{4.95}Mn_{6.05}$ and $CeCo_8Mn_3$ exhibits properties characteristic of a canted antiferromagnetic state.

1. Introduction

Rare earth-based compounds are widely used as permanent magnets, one example of this is the most powerful large scale commercially produced magnet $Nd_2Fe_{14}B$ [1]. As Ce is the most abundant rare-earth element [2], there has been substantial effort to develop permanent magnets based on Ce [3–6]. Most recent attention has been given to Ce–transition metal compounds based on the $ThMn_{12}$ (1:12) [5,6], and (H)–Th_2Ni_{17} structure types (2:17). As the transition metal elements of Mn, Fe and Co all carry magnetic moments, the decision was made to study structural and magnetic properties of alloys in the Ce–T–Mn (T = Fe, Co) systems, where the hexagonal 2:17 phases were reported [7,8].

The phase diagram of the Ce–Fe–Mn system was first experimentally investigated by X-ray diffraction (XRD) at 400 °C and 600 °C in 1974 [7]. A more detailed study on the $ThMn_{12}$ phases was published in 1976 by the same team [9] and in 2016 a new phase diagram was presented by Fartushna et al. [8,10] based on differential thermal analysis (DTA), XRD, scanning electron microscopy (SEM) and electron probe microanalysis (EPMA). In general, these works complement each other well, though some differences occur in the homogeneity ranges and the solidus/liquidus transitions due to the different temperatures used in the respective studies. In both cases, existence of the two ternary $Ce_2Fe_{11}Mn_6$ and $CeFe_5Mn_7$ compounds was reported with the (H)–Th_2Ni_{17}-type and $ThMn_{12}$-type structures, respectively.

The phase diagram of the Ce–Co–Mn system was experimentally investigated at 400 °C and 600 °C by XRD, DTA and microstructural analysis. In addition to the other ternary compounds observed in the Ce–Co–Mn system, formation of the 2:17 ($Ce_2Co_{14.11}Mn_{2.89}$) compound with (H)–Th_2Ni_{17}-type structure has been observed [11]. The $Ce_2Co_{12}Mn_5$ compound, which also has a stoichiometric 2:17 composition, was reported with an unknown structure [11]. Furthermore, the phase diagrams of the Ce–T–Mn (T = Ni, Cu) systems [12,13] were studied by the same group, with the same methods and temperature ranges previously used for the Ce–Fe–Mn system [7]. However, neither binary nor ternary 2:17 compounds of the (H)–Th_2Ni_{17}-type structure in the Ce–T–Mn

* Corresponding author.
E-mail address: martin.sahlberg@kemi.uu.se (M. Sahlberg).

https://doi.org/10.1016/j.jallcom.2020.157435

(T = Ni, Cu) systems were reported.

The study was initially prompted by a desire to understand the magnetic properties of Ce–Fe–Mn ternary phases, mainly τ_1 ($Ce_2Fe_{11}Mn_6$, Th_2Ni_{17} structure type) and τ_2 ($CeFe_5Mn_7$, $ThMn_{12}$) which have not been described in the literature before. The τ_2 phase was successfully synthesized without any issues. However, when trying to synthesize τ_1 it was never possible to index all peaks of the diffractograms to the Th_2Ni_{17} structure. After scrutinizing the data, it was found that it could be indexed as the $Nd_3(Fe,Ti)_{29}$ structure. It was decided to investigate several Ce–T–Mn alloys, including an unknown structure in the Ce–Co–Mn system and report magnetic properties of new members in these systems. It is worthwhile to mention that in the Ce–T–Mn (T = Fe, Co) systems, the existence of the hexagonal 2:17 phases was studied with some homogeneity regions. Due to this, the impact of the Fe/Mn and Co/Mn concentration on the magnetic properties was also investigated.

In this study, new findings are presented on the Ce–T–Mn (T = Fe, Co) systems [10,11] based on a careful analysis of the original data, mainly regarding the T rich (T = Fe, Co) part of the phase diagram. This is done by XRD, elemental dispersive spectroscopy (EDS) and superconducting quantum interference device (SQUID) magnetometry on samples produced by our group and supported by extensive literature studies, not only limited to Ce–T–T' systems, but also those of R–T–T'. The crystal structures of the new Ce-based ternary compounds and their magnetic properties are presented below.

2. Experimental details

The Ce–T–Mn (T = Fe, Co, Ni) samples were synthesized using arc-melting of high purity Ce and Mn (99.9%), Fe, Co and Ni (99.99%) from Alfa Aesar. Oxygen contamination was minimized by flushing the furnace five times with Ar (purity 99.999%) and by melting a Ti getter prior to melting the sample. The samples were turned over and remelted three times to promote homogeneity. Negligible losses of Mn (<1 wt%) were detected in most cases. In the event of larger losses, more Mn (1–3 wt%) was added to compensate as only Mn evaporates in these alloys during arc melting. The samples were wrapped in Ta-foil, placed in a quartz tube and sealed under vacuum for later annealing at 1000, 900 and 800 °C for 75, 100 and 125 h, respectively. Afterwards samples were quenched in cold water. All samples were characterized using a Bruker D8 X-ray diffractometer with a Lynx-eye position sensitive detector and Cu-Kα radiation on a zero-background single crystal Si sample holder. Phase analysis and structural refinement of the X-ray data using the Rietveld-method were done by the FullProf Suite software [14].

The microstructure was evaluated with a Zeiss Merlin SEM equipped with a secondary electron (SE) detector and an energy-dispersive X-ray spectrometer (EDS). The samples for electron microscopy analysis were prepared by standard metallographic techniques through grinding with SiC paper. For the final polishing, a mixture of SiO_2 and H_2O was used.

Magnetic measurements as function of temperature were carried out in an MPMS XL SQUID using a field cooled protocol (FC) with 8 kA/m as the probing field, as well as a function of applied magnetic field up to 1.6 MA/m at various temperatures. The temperature range was limited to between 10 and 390 K.

3. Results and discussion

Initial attempts to synthesize the hexagonal 2:17 Ce–Fe–Mn compounds were based on the methods used in Refs. [8,10]. Ta-foil was used instead of Al_2O_3 crucibles, as attempts to anneal in Al_2O_3 resulted in oxidation due to interaction with the crucibles. For systems with Co and Ni the annealing temperature was lowered to avoid liquid state of the alloys. Ni-containing samples have been synthesized to compare magnetic properties of the 1:11 compounds with Co- and Cu-containing compounds [15]. The composition of the Ce–T–Mn (T = Fe, Co, Ni) alloys, annealing temperature, XRD phase analysis and EDS compositions are presented in Table 1.

3.1. On the 3:29 phase in the Ce–Fe–Mn system

Several alloys along the homogeneity region of the $Ce_2Fe_{11}Mn_6$ compound [10] have been synthesized. Alloy syntheses were repeated several times to verify synthesis conditions, reduce oxide formation and to confirm phase equilibria. In some cases, small amounts of oxides were detected, and were taken into account when evaluating the phase equilibria and compositions. It was deduced that these small amounts of oxides did not significantly influence the overall results. No signs hinting to the existence of compounds with (H)–Th_2Ni_{17} structure type have been found (Table 1). The 1:12 phase on the contrary has been easily identified in most cases, but additional observed peaks could not be fitted to any of the possible binary compounds. To verify the synthesis method, the compound $Ce_2Fe_{15}Mn_2$ was chosen as it is well known in literature [16]. This compound was found to have the (R)-Th_2Zn_{17} structure type reported previously [7–10]. The only reported disparity appears in Ref. [10], where a diffractogram for the $Ce_2Fe_{11}Mn_6$ compound with the (H)–Th_2Ni_{17} structure type was presented. Attempts to promote either of the (H)–Th_2Ni_{17} (low temperature modification) or (R)-Th_2Zn_{17} (high temperature modification) phases in the samples by annealing at temperatures of 900 or 1000 °C were unsuccessful. The samples appeared to be either multiphase or compounds with new structures containing several low intensity superlattice peaks. To explain these unresolved peaks, the region of the phase diagram containing τ_1 ($Ce_2Fe_{11}Mn_6$, Th_2Ni_{17} structure type) and τ_2 ($CeFe_5Mn_7$, $ThMn_{12}$) [7–10] phases was investigated, in an effort to uncover any obscure Fe-rich structures which might agree with the data.

Looking to the literature in the Crystal Structure Database for Inorganic Compounds [17] for the Ce-based ternary systems, only 21 compounds with (H)–Th_2Ni_{17} structure type have been reported. A compound which seemed to be in good agreement with the diffractogram was found in the Fe-rich family and relates to the $Nd_3Fe_{29-x}Ti_x$ (3:29) type structure [18]. Nearly all peaks from the experimental diffractogram were fitted according to this model, in contrast to 2:17 [11]. It is worthwhile to note that according to this database only 175 representatives of this structure type exist and only one containing Mn ($Nd_3Fe_{18.5}Mn_{10.5}$ [19]).

The $Ce_2Fe_{11}Mn_6$ alloy, annealed at 1000 °C, was used for the detailed structural investigation. Crystallographic parameters of the $Ce_3Fe_{24.94}Cr_{4.06}$ compound (space group $C2/m$) [20] have been used as starting parameters for the crystal structure refinement of the new $Ce_3(Fe_{0.638}Mn_{0.362})_{29}$ compound. As Fe and Mn are hard to differentiate when using X-ray analysis some considerations had to be taken when refining the data. The general approach was to put Fe and Mn in the positions where the best R-factors can be found with a reliable displacement parameter (B_{iso}). Using concentrations of Fe and Mn that agree with EDS results as well as the assumption that Mn, like Cr, does not enter 4*g*, 4*e* and 2*c* positions, and only substitutes Fe in 4*i* and 8*j* positions. This is based on results from Mössbauer spectroscopy of the $Tb_3Fe_{29-x}Cr_x$ compound [21]. With these considerations, reliable values of R-factors have been found following the Rietveld refinement: R_{Bragg} = 4.05%, R_f = 2.81% and χ^2 = 6.10. The final Rietveld refinement was based on the only known neutron results for the 3:29 phase: the compound $Nd_3Fe_{27.695}Ti_{1.305}$ (space group $P2_1/c$) [18]. The choice of refinement

Table 1
Results of the phase analysis in the Ce–*T*–Mn (*T* = Fe, Co, Ni) alloys.

Alloy	$T_{annealing}$ (°C)	Phase	Structure type/Space group	Cell parameters (Å)			β for the 3:29 phase (°)	Phase content (wt %)	EDS composition (at.%)
				a	b	c			
Ce–Fe–Mn system									
$Ce_2Fe_{11}Mn_6$	900	$Ce_3(Fe,Mn)_{29}$	$Nd_3(Fe,Ti)_{29}/P2_1/c$	10.5803(8)	8.5488(5)	9.7008(7) 4.7602(2) 96.842(5)	53.2	$Ce_{9.9}Fe_{59.7}Mn_{30.4}$	
		$Ce(Fe,Mn)_{12}$	$ThMn_{12}/I4/mmm$	8.5361(3)			36.4	$Ce_{8.8}Fe_{60.2}Mn_{30.0}$	
		$Ce(Fe,Mn)_2$	$MgCu_2/Fd\bar{3}m$	7.3725(4)			10.4	–	
$Ce_2Fe_{11}Mn_6$	900	$Ce_3(Fe,Mn)_{29}$	$Nd_3(Fe,Ti)_{29}/P2_1/c$	10.5570(5)	8.5263(4)	9.6823(4) 6.048(1) 96.833(2)	95.1	$Ce_{9.7}Fe_{55.7}Mn_{34.6}$	
		$Ce(Fe,Mn)_2$	$MgCu_2/Fd\bar{3}m$	7.3443(5)			3.7	$Ce_{32.2}Fe_{43.4}Mn_{24.4}$	
		Ce_2O_3	$La_2O_3/P\bar{3}m1$	3.8895(5)			1.2	–	
$Ce_2Fe_{13}Mn_4$	1000	$Ce_3(Fe,Mn)_{29}$	$Nd_3(Fe,Ti)_{29}/P2_1/c$	10.5601(2)	8.5213(2)	9.6809(2) 12.4392(4) 96.850(1)	64.2	$Ce_{9.8}Fe_{68.0}Mn_{22.2}$	
		$Ce_2(Fe,Mn)_{17}$	$Th_2Zn_{17}/R\bar{3}m$	8.5206(2)			35.4	$Ce_{10.8}Fe_{71.9}Mn_{17.3}$	
		CeO_2	$CaF_2/Fm\bar{3}m$	5.642(1)			0.4	–	
$Ce_2Fe_{15}Mn_2$	900	$Ce_2(Fe,Mn)_{17}$	$Th_2Zn_{17}/R\bar{3}m$	8.4914(3)		12.4049(4)	97.1	–	
		α-Fe	$W/Im\bar{3}m$	2.8734(6)			2.9	–	
$CeFe_8Mn_4$	900	$Ce_3(Fe,Mn)_{29}$	$Nd_3(Fe,Ti)_{29}/P2_1/c$	10.5748(2)	8.5395(1)	9.6964(2) 5.120(3) 96.847(2)	85.9	$Ce_{9.9}Fe_{68.5}Mn_{21.4}$	
		(γ-Fe,Mn)	$Cu/Fm\bar{3}m$	3.6152(2)			10.4	$Ce_{2.1}Fe_{72.4}Mn_{25.5}$	
		$Ce(Fe,Mn)_{12}$	$ThMn_{12}/I4/mmm$	8.431(5)			3.7	$Ce_{8.2}Fe_{59.3}Mn_{32.5}$	
$Ce_2Fe_{11}Mn_6$	1000	$Ce_3(Fe,Mn)_{29}$	$Nd_3(Fe,Ti)_{29}/P2_1/c$	10.5789(1)	8.5424(1)	9.6940(1) 96.879(1)	98.3	$Ce_{9.7}Fe_{57.5}Mn_{32.8}$	
		CeO_2	$CaF_2/Fm\bar{3}m$	5.463(1)			1.7	$Ce_{\sim 32.1}O_{\sim 67.9}$	
Ce–Co–Mn system									
$Ce_2Co_{12}Mn_5$	800	$Ce(Co,Mn)_{11}$	$Ce(Mn,Ni)_{11}/P4/mbm$	8.2105(3)		4.7266(2)	91.6	$Ce_{9.2}Co_{62.5}Mn_{28.3}$	
		$Ce(Co,Mn)_{12}$	$ThMn_{12}/I4/mmm$	8.568(1)		4.735(1)	8.4	$Ce_{8.8}Co_{61.8}Mn_{29.4}$	
$Ce_2Co_{13}Mn_4$	800	$Ce(Co,Mn)_{11}$	$Ce(Mn,Ni)_{11}/P4/mbm$	8.2014(2)		4.7163(1)	86.6	–	
		$Ce_2(Co,Mn)_7$	$Ce_2Ni_7/P6_3/mmc$	4.9634(2)		24.513(2)	13.4	–	
$Ce_2Co_{14}Mn_3$	800	$Ce_2(CoMn)_{17}$	$Th_2Zn_{17}/R\bar{3}m$	8.4272(1)		12.3290(2)	81.7	$Ce_{10.5}Co_{73.4}Mn_{16.1}$	
		$Ce(Co,Mn)_{11}$	$Ce(Mn,Ni)_{11}/P4/mbm$	8.1935(3)		4.7053(3)	18.3	$Ce_{8.8}Co_{69.1}Mn_{22.1}$	
$Ce_3Co_{21}Mn_8$	800	$Ce(Co,Mn)_{11}$	$Ce(MnNi)_{11}/P4/mbm$	8.2027(2)		4.7150(1)	96.2	$Ce_{9.2}Co_{65.2}Mn_{25.6}$	
		$Ce_2(Co,Mn)_7$	$Ce_2Ni_7/P6_3/mmc$	4.9640(4)		24.520(5)	3.8	$Ce_{21.0}Co_{65.7}Mn_{13.3}$	
Ce–Ni–Mn system									
$CeNi_{4.95}Mn_{6.05}$	800	$Ce(Ni,Mn)_{11}$	$Ce(MnNi)_{11}/P4/mbm$	8.3573(2)		4.9182(1)	94.6	$Ce_{8.5}Ni_{40.4}Mn_{51.1}$	
		$Ce(Ni,Mn)_{12}$	$ThMn_{12}/I4/mmm$	8.547(1)		4.721(1)	5.0	$Ce_{7.3}Ni_{39.6}Mn_{53.1}$	
		Ce_2O_3	$La_2O_3/P\bar{3}m1$	3.893(2)		6.072(5)	0.4	–	
$CeNi_5Mn_7$	800	$Ce(Ni,Mn)_{11}$	$Ce(MnNi)_{11}/P4/mbm$	8.3667(2)		4.9225(1)	93.3	$Ce_{8.6}Ni_{37.7}Mn_{53.7}$	
		$Ce(Ni,Mn)_{12}$	$ThMn_{12}/I4/mmm$	8.5509(9)		4.7235(8)	6.7	$Ce_{7.2}Ni_{36.2}Mn_{56.6}$	

is based on neutrons being the best method to separate electronically similar elements such as Fe and Mn. In the final model higher symmetry and slightly better R-factors were achieved: $R_{Bragg} = 3.77\%$, $R_f = 2.79\%$ and $\chi^2 = 5.66$. As in the previous model there are several equal 4*e* positions, Fe/Mn have been distributed according to the EDS results in random concentration and in consideration of B_{iso}. It was found that ten 4*e* positions are filled by Fe and Mn in proportions of 0.5 + 0.5 and in one case 0.75 + 0.25, as seen in Table 2. All other positions are related only to Fe or Ce resulting in the $Ce_3(Fe_{0.638}Mn_{0.362})_{29} = Ce_3Fe_{18.5}Mn_{10.5}$ composition, similar to that of $Nd_3Fe_{18.5}Mn_{10.5}$. A more ordered model could not be rejected of course, but the presented structure has the best R-factors and positive atomic displacement. Moreover, the positions with larger values of the coordination numbers *M*4, *M*9 and *M*10 are more acceptable for the larger Mn atoms, as can be seen from the Table 2. Attempts to fix elements to certain positions to enforce an ordered structure resulted in all other parameters deteriorating. Furthermore, in the ordered structure it was hard to separate B_{iso} for Fe and Mn as they are almost in the same range (1.2–1.5 Å^2) after this procedure. To clarify the Fe/Mn distribution, neutrons are needed. The XRD pattern and SEM image of the $Ce_2Fe_{11}Mn_6$ sample are shown in Fig. 1 and the obtained structural parameters for the new $Ce_3(Fe_{0.638}Mn_{0.362})_{29}$ compound are presented in Table 2.

The unit cell projection onto the *ca* plane together with coordination polyhedra of the atoms in $Ce_3(Fe_{0.638}Mn_{0.362})_{29}$ are shown in Fig. 2. For clear interpretation, only selected polyhedra are presented as others are repeated. Both Ce1 and Ce2 atoms are surrounded by 20 atoms forming the pseudo Frank-Kasper coordination polyhedron (Ce1@Fe_6M_{14} and Ce2@$CeFe_4M_{15}$). Most Fe and Fe/Mn (*M*) atoms are surrounded by 12 atoms forming an icosahedron (Fe1, Fe3, *M*7, *M*8 and *M*11@$Ce_2Fe_2M_8$; Fe2 and *M*2@Ce_3FeM_8; *M*1@$Ce_2Fe_4M_6$; *M*3, *M*4 and *M*6@$Ce_2Fe_3M_7$; *M*5@$Ce_3Fe_3M_6$). The rest of the Fe and *M* atoms are surrounded by 14 atoms forming the 14-vertex Frank-Kasper polyhedron (Fe4@$CeFe_3M_{10}$; *M*9 and *M*10@$CeFe_4M_9$). The shortest Ce–Ce, Ce–Fe, Ce–*M*, Fe–*M*, Fe–Fe and *M*–*M* distances are 3.830(2), 3.076(3), 2.959(9), 2.327(15), 2.401(5) and 2.362 (15) Å, respectively. These values are close to the sum of the atomic radii ($r_{Ce} = 1.82$, $r_{Fe} = 1.26$, $r_{Mn} = 1.27$ Å [22]). The list of interatomic

Table 2
Results of the crystal structure refinement of the new $Ce_3(Fe_{0.638}Mn_{0.362})_{29}$ and $CeCo_8Mn_3$ ternary compounds.

Atom	Site	x	y	z	B_{iso} (Å^2)
3:29 phase					
Calculated composition: $Ce_3(Fe_{0.638}Mn_{0.362})_{29} = Ce_3Fe_{18.5}Mn_{10.5}$					
$Nd_3(Fe,Ti)_{29}$-type, sp. gr. $P2_1/c$ (No. 14), a = 10.57508(10) Å, b = 8.53957(7) Å, β = 96.877(1)°, c = 9.69154(9) Å, V = 868.913(14) Å^3, Z = 2					
R_{Bragg} = 3.78%, R_f = 2.79%					
Ce1	2*a*	0	0	0	1.5(1)
Ce2	4*e*	0.4060(2)	0.0019(8)	0.8184(2)	1.4(1)
Fe1	2*d*	1/2	0	1/2	1.4(2)
Fe2	4*e*	0.5994(8)	0.2366(9)	0.4280(10)	0.5(2)
Fe3	4*e*	0.9901(9)	0.2551(13)	0.2408(11)	1.0(1)
Fe4	4*e*	0.0075(11)	0.3600(4)	0.0087(11)	0.8(1)
*M*1	4*e*	0.1111(4)	0.999(2)	0.7269(4)	1.4(1)
*M*2	4*e*	0.2885(5)	0.997(2)	0.0923(5)	1.5(1)
*M*3	4*e*	0.6234(8)	0.1484(12)	0.6793(11)	1.0(2)
*M*4	4*e*	0.8014(9)	0.2212(11)	0.0912(12)	1.9(3)
*M*5	4*e*	0.4150(8)	0.2454(9)	0.0676(11)	1.3(3)
*M*6	4*e*	0.8052(9)	0.2463(12)	0.8490(10)	1.2(2)
*M*7	4*e*	0.2013(8)	0.2583(12)	0.1619(11)	1.1(2)
*M*8	4*e*	0.3668(9)	0.3637(12)	0.8120(11)	1.2(2)
*M*9	4*e*	0.2552(4)	0.005(2)	0.5208(4)	1.6(1)
*M*10	4*e*	0.1383(4)	0.004(2)	0.2941(5)	1.8(1)
*M*11	4*e*	0.1991(9)	0.2873(11)	0.4115(11)	1.0(2)
From *M*1 to *M*10: *Mn* = 0.5Fe + 0.5Mn and *M*11 = 0.75Fe + 0.25Mn					
1:11 phase					
Calculated composition: $CeCo_8Mn_3$					
$Ce(Mn,Ni)_{11}$-type, sp. gr. $P4/mbm$ (No. 127), a = 8.20302(9) Å, c = 4.71524(6) Å, V = 317.286(7) Å^3, Z = 2					
R_{Bragg} = 7.01%, R_f = 5.46%					
Ce	2*a*	0	0	0	1.28(3)
Co1	8*k*	0.1796(2)	*x*+1/2	0.2426(4)	0.87(4)
Co2	8*j*	0.0647(1)	0.2124(1)	1/2	0.37(4)
Mn1	4*g*	0.6146(2)	*x*+1/2	0	0.42(6)
Mn2	2*c*	0	1/2	1/2	0.68(6)

distances is given in Supporting Information (Table S1).

To support the results of the X-ray findings, EDS analysis has been used to determine the composition of the new compound and find its corresponding homogeneity region. It was found that the experimentally observed compositions were all accurate within 1–2 at.%. The Ce content is generally overestimated (Table 1). From the crystal structure of the 3:29 phase, the Ce content should be 9.375 at.%, but the results indicate 9.8 ± 0.1 at.%. This discrepancy has been observed previously [8,10] and it is difficult to assign this to an instrumental error or deviation from the homogeneity region of the 3:29 phase. For instance, a compound with the composition of $Ce_{1.56}Fe_{8.84}Cr_{2.60}$ [23] was reported instead of $CeFe_9Cr_3$. The homogeneity region of the 3:29 phase, according to the present study has been defined as follows: from $Ce_{9.7}Fe_{55.7}Mn_{34.6}$ to $Ce_{9.9}Fe_{68.5}Mn_{21.4}$ (indexes are in atomic percentages). Composition of this compound can be presented as $Ce_{3+x}(Fe,Mn)_{29}$ after a detailed neutron scattering study. It is close enough to the results for 2:17 phase ((H)–Th_2Ni_{17}-type) [10] but crystal structure findings dispute this. In the end, the 2:17 phase ((R)-Th_2Zn_{17}-type) dissolves up to ~17 at.% of Mn which is in agreement with literature [16].

3.2. On the 1:11 phase in the Ce–Co–Mn system

As mentioned above, the $Ce_2Co_{14.11}Mn_{2.89}$ compound with a (H)–Th_2Ni_{17} structure type has been reported previously [11]. However, from the synthesis procedure described here previously, a two-phase $Ce_2Co_{14}Mn_3$ alloy was observed (Table 1). There is a 2:17 phase, but rather than being hexagonal (Th_2Ni_{17}) it is rhombohedral (Th_2Zn_{17}). Nevertheless, Sun et al. observed $Ce_2Co_{17-x}Mn_x$ (x = 0–4) compounds with the (H)–Th_2Ni_{17} structure type [24]. The results on the presence of the phase with (R)-Th_2Zn_{17}-type structure in the $Ce_2Co_{14}Mn_3$ alloy do however, agree well with $Ce_2Co_{15}Mn_3$ [25].

The $Ce_2Co_{12}Mn_5$ compound which was reported with unknown structure has also been synthesized in the present study. From our findings in the Ce–Fe–Mn system and because of the $Sm_3Co_{21.5}Cr_{7.5}$ structure [26], an alloy with the composition $Ce_3Co_{21}Mn_8$ was prepared as well. The new compound $Ce(Co,Mn)_{11}$ was observed in both cases. It has tetragonal space group ($P4/mbm$) with the $Ce(Ni,Mn)_{11}$ prototype. It is worthwhile to note that according to the Crystal Structure Database for Inorganic Compounds only 23 representatives of this structure type exist, with only one of these containing Co ($GdTi_2Fe_{6.3}Co_{2.7}$). The nominal composition of our Co-containing compound is Mn poor $CeCo_8Mn_3$ (25 at.%) as compared to $CeNi_5Mn_6$ (50 at.%). The lower content of Mn in the new compound explains the smaller unit cell volume compared to the known compound (317.26 *vs*. 342.80 Å^3). Indeed $CeCu_{8.75}Mn_{2.25}$ [15] has the same structure and is from the same homogeneity region as the new Co-containing compound. The compound with Ni is completely disordered. The compound with Cu exhibits some ordering, observed by single crystal studies and the same feature is true for the Co compound.

XRD data have been collected for the $Ce_3Co_{21}Mn_8$ alloy and used for the detailed structural investigation of the new 1:11 phase. Crystallographic parameters of the $CeCu_{8.75}Mn_{2.25}$ compound have been used as the starting model for the refinement. The Co-containing compound has a smaller cell volume compared to the known compound with Cu (317.26 *vs*. 350.39 Å^3), which is probably due to Co having a smaller atomic radius than Cu. Atoms of Ce are located in the 2*a* position. As mentioned previously, due to the difficulty of differentiating between Mn, Co, Fe, Ni and Cu using X-rays, compositional adjustment has been used according to the EDS and positive atomic displacement. According to the refinement, Mn and Co fully occupy 2*c* and 4*g*, and 8*k* and 8*j* positions, respectively. Resulting in the final formula of the new compound being $CeCo_8Mn_3$. A disordered model could not be rejected of course, but an ordered variant provided the best R-factors while also having positive atomic displacement.

Projection of the $CeCo_8Mn_3$ unit cell on the *ba*-plane and coordination polyhedra of the atoms are presented in Fig. 2. The atomic surrounding of Ce is characterized by the Pseudo Frank-Kasper coordination polyhedra with coordination number (*CN*) 20 ($Ce@Co_{16}Mn_4$). All Co atoms have icosahedral coordination with *CN* = 12 ($Co1@Ce_2Co_6Mn_4$ and $Co2@Ce_2Co_7Mn_3$). One Mn atom is located in the center of the icosahedron ($Mn2@Co_8Mn_4$) with *CN* 12, while another is in the 15-vertex Frank-Kasper polyhedron ($Mn1@Ce_2Co_{10}Mn_3$). The shortest Ce–Co, Ce–Mn, Co–Mn, Co–Co and Mn–Mn distances are 2.979(1), 3.298(2), 2.411(2), 2.288(3) and 2.659(2) Å, respectively. Their values are close to the sum of the atomic radii (r_{Ce} = 1.82, r_{Co} = 1.25, r_{Mn} = 1.27 Å [22]). The list of interatomic distances is given in Table S2.

The homogeneity region for the 1:11 phase has been defined based on the EDS results. As previously observed for Fe-containing samples, deviation of Ce content is also noted (9.07 ± 0.13 at.% instead of 8.3 at.%.). The homogeneity region of the 1:11 phase according to our results has been defined as follows: from $Ce_{9.2}Co_{62.5}Mn_{28.3}$ to $Ce_{8.8}Co_{69.1}Mn_{22.1}$ (indexes are in atomic percentages). Deviation of Ce in the Ce–Co–Mn system is common, as according to the phase equilibria [11] a reasonable deviation in Ce concentration has been observed for $Ce_{1-y}Co_{3-x}Mn_x$. Composition of the studied compound in this work can be presented as $Ce_{1+x}(Co,Mn)_{11}$ after a detailed neutron scattering study. According to the EDS results for the $Ce_2Co_{14}Mn_3$ alloy, the Ce_2Co_{17} phase can dissolve up to ~16 at.% of Mn. This means that the solid solution based on the Ce_2Co_{17} binary compound cover the proposed individual ternary $Ce_2Co_{14.11}Mn_{2.89}$ compound [11]. It is worthwhile to

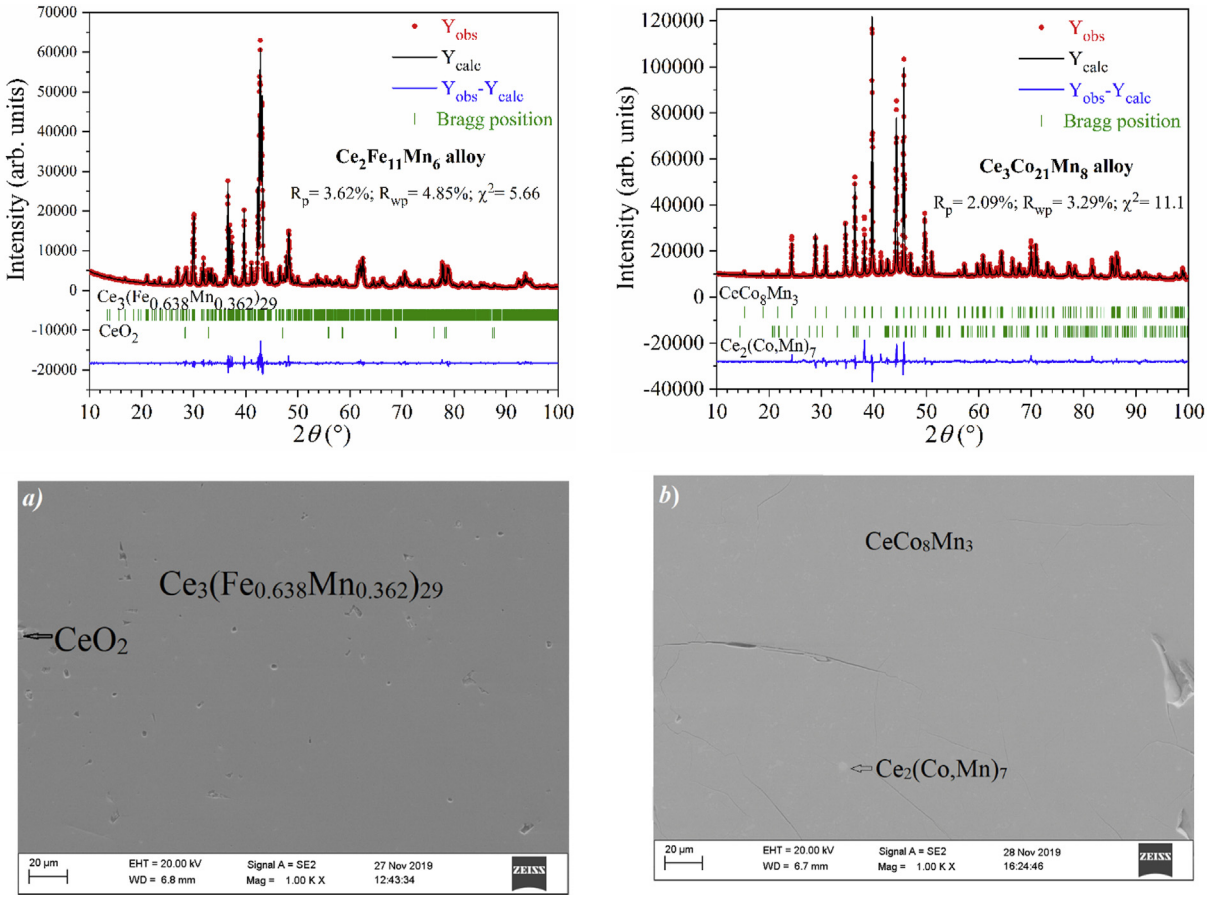

Fig. 1. The XRD patterns with the results of the Rietveld refinement and SEM of the $Ce_2Fe_{11}Mn_6$ annealed at 1000 °C (a) and $Ce_3Co_{21}Mn_8$ annealed at 800 °C (b) alloys. Phases which were observed in alloys are presented on diffractograms (near Bragg position) and on SEM-images.

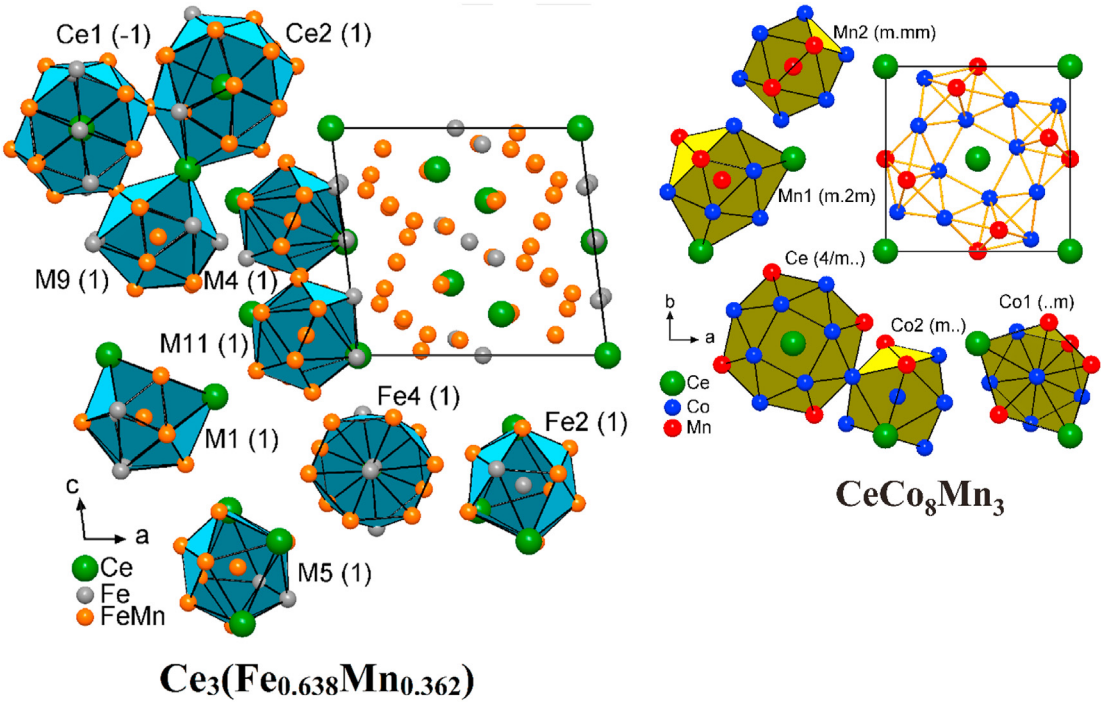

Fig. 2. Projection of the $Ce_3(Fe_{0.638}Mn_{0.362})_{29}$ and $CeCo_8Mn_3$ unit cell on the *ca* and *ba* plane, respectively and coordination polyhedra of the atoms. Symmetries of the central atoms are indicated in parentheses.

note that in the Ce–Ni–Mn system deviation of Ce is less than in the Ce–*T*–Mn (*T* = Fe, Co), see Table 1.

3.3. Discussion of the crystal structure peculiarities in the Ce–T–Mn (T = Fe, Co, Ni, Cu) systems

Here we would like to emphasize the exceptionally narrow range for the existence of the ternary compounds in the *T*-rich region of the Ce–*T*–Mn (*T* = Fe, Co, Ni, Cu) systems (Fig. 3). For instance, the difference between 2:17 and 3:29 phases is only ~1 at.% of Ce. Microscopic techniques give errors of around 1–2 at.% which is why some compounds can be obscured in this way. The 1:11, 1:12 and 3:29 binaries do not exist or they are metastable. Only stabilized ternary variants found bigger distribution. Usually solid solutions form based on the binary 1:2, 1:3, 1:5, 1:6, 2:7, 2:17 and 5:19 compounds in the Ce–*T*–Mn (*T* = Fe, Co, Ni, Cu) systems. As can be seen from the Ce–*T*–Mn (*T* = Fe, Co, Ni, Cu) systems, one experimental technique is not enough to investigate the phase diagram or crystal structure of the new compounds. Moreover, updates (especially to the Ce–*T*–Mn (*T* = Fe, Co) phase diagrams) are needed as new compounds were discovered in this study.

Detailed structural discussion on the peculiarities of the 1:12, 2:17 and 3:29 phases are well presented in paper [27] and graphical comparisons of the experimental diffractograms can be found in Ref. [19].

The 3:29 structure type is an intermediate between the tetragonal $ThMn_{12}$ and the rhombohedral (R)-Th_2Zn_{17} ($R\bar{3}m$ *h*) and its crystal structure is of lower symmetry, $C2/m$ or $P2_1/c$ rather than the (H)–Th_2Ni_{17} ($P6_3/mmc$). As early as 1968, Johnson and Smith [28] discussed structures that, in modern notation, could be derived from the $CaCu_5$ structure. The process is that a fraction, δ, of the Ca atoms are substituted by a pair of transition metals, *T* as $Ca_{1-\delta}(2T)_\delta Cu_5$ - > CaT_z, where $\delta = \frac{z-5}{z+2}$. In this case, $\delta = \frac{1}{2}$ corresponds to 1:12, $\delta = \frac{1}{3}$ corresponds to 2:17 and $\delta = \frac{2}{5}$ corresponds to the 3:29 structure. However, this does not mean that all rational values of δ will give new unique structures, some will be of another crystal structure already described by other means. Another point of note is that δ cannot exceed $\frac{1}{2}$ since the interatomic distance would be too short.

Following Han et al. [29] the following vector transformations can be done in reciprocal space

$$\begin{cases} \begin{pmatrix} h \\ k \\ l \end{pmatrix}_{1:12} = \begin{pmatrix} 1 & -1 & 0 \\ 0 & 0 & 2 \\ -1 & -1 & 0 \end{pmatrix} \begin{pmatrix} h \\ k \\ l \end{pmatrix}_{1:5} \\ \begin{pmatrix} h \\ k \\ l \end{pmatrix}_{2:17} = \begin{pmatrix} -1 & -2 & 0 \\ 2 & 1 & 0 \\ 0 & 0 & 2 \end{pmatrix} \begin{pmatrix} h \\ k \\ l \end{pmatrix}_{1:5} \\ \begin{pmatrix} h \\ k \\ l \end{pmatrix}_{3:29} = \begin{pmatrix} -2 & -2 & 1 \\ 1 & -1 & 0 \\ 1 & 1 & 2 \end{pmatrix} \begin{pmatrix} h \\ k \\ l \end{pmatrix}_{1:5} \end{cases},$$

where the Miller indices of 1:5 relates to the type structure $CaCu_5$. This means that most of the indices found in the 3:29 structure have a corresponding one in the 2:17 and 1:12 structure. However, as an example, the index of (3 2 2) in the 3:29 crystal structure does not correspond to any reflection in the 1:12 or 2:17 systems since it gives Miller indices which are not whole numbers, but rather rational numbers, *e.g.*

$$\begin{pmatrix} 3 \\ 2 \\ 2 \end{pmatrix}_{3:29} = \begin{pmatrix} 2 \\ \frac{14}{5} \\ \frac{4}{5} \end{pmatrix}_{1:12} = \begin{pmatrix} \frac{11}{5} \\ -\frac{1}{5} \\ \frac{14}{5} \end{pmatrix}_{2:17}.$$

Aside from the compositional neighborhood, the structure of 3:29 compound is clearly related to the structures of 1:12 and 2:17 phases. In general 1:11 compounds (Fig. 3) have the $Ce(Ni_{0.45}Mn_{0.55})_{11}$-type structure (the YNi_9In_2 structure type is an ordered superstructure to the $Ce(Ni_{0.45}Mn_{0.55})_{11}$-type) and they are closely related to the 1:12 phase. Alternatively, all structures can be presented as a $CaCu_5$–Zr_4Al_3 intergrowth [12,27].

3.4. Magnetism of the new 3:29 and 1:11 phases

As previously discussed, $CeNi_{4.95}Mn_{6.05}$ (1:11), corresponds to a disordered structure from a crystallographic point of view in terms of Ni and Mn positions in the crystal structure. The low field magnetization versus temperature result shown in Fig. 4(a) indicates the onset of a canted antiferromagnetic state at a temperature of about 300 K. In addition, there is a cusp at approximately

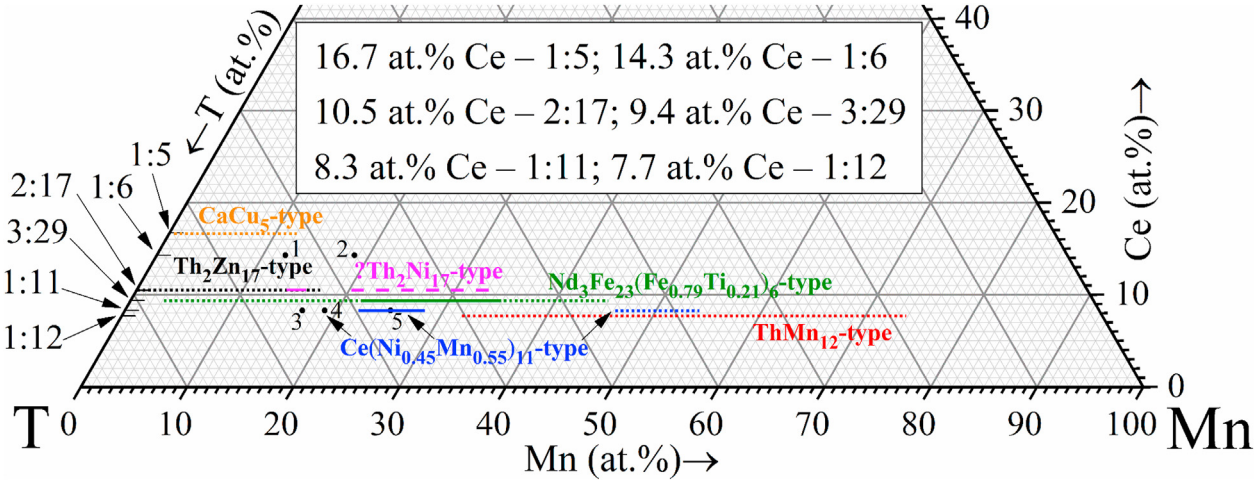

Fig. 3. Schematic representation of the compositional range of existence of different structure types in the Ce–*T*–Mn (*T* = Fe, Co, Ni, Cu) systems. Solid lines – compositional ranges found or confirmed in this investigation. Dotted lines – compositional ranges according to the literature database [17]. Dashed line – region of the Th_2Ni_{17}-type compounds. Circles – compounds with constant composition: 1 – $CeCu_{5.15}Mn_{0.85}$ ($CeCu_5Au$-type), 2 – $CeCu_{4.7}Mn_{1.3}$ ($YbMo_2Al_4$-type), 3 – (YNi_9In_2-type), 4 – $CeCu_{8.75}Mn_{2.25}$ ($Ce(Ni_{0.45}Mn_{0.55})_{11}$-type) and 5 – $CeCo_8Mn_3$ ($Ce(Ni_{0.45}Mn_{0.55})_{11}$-type).

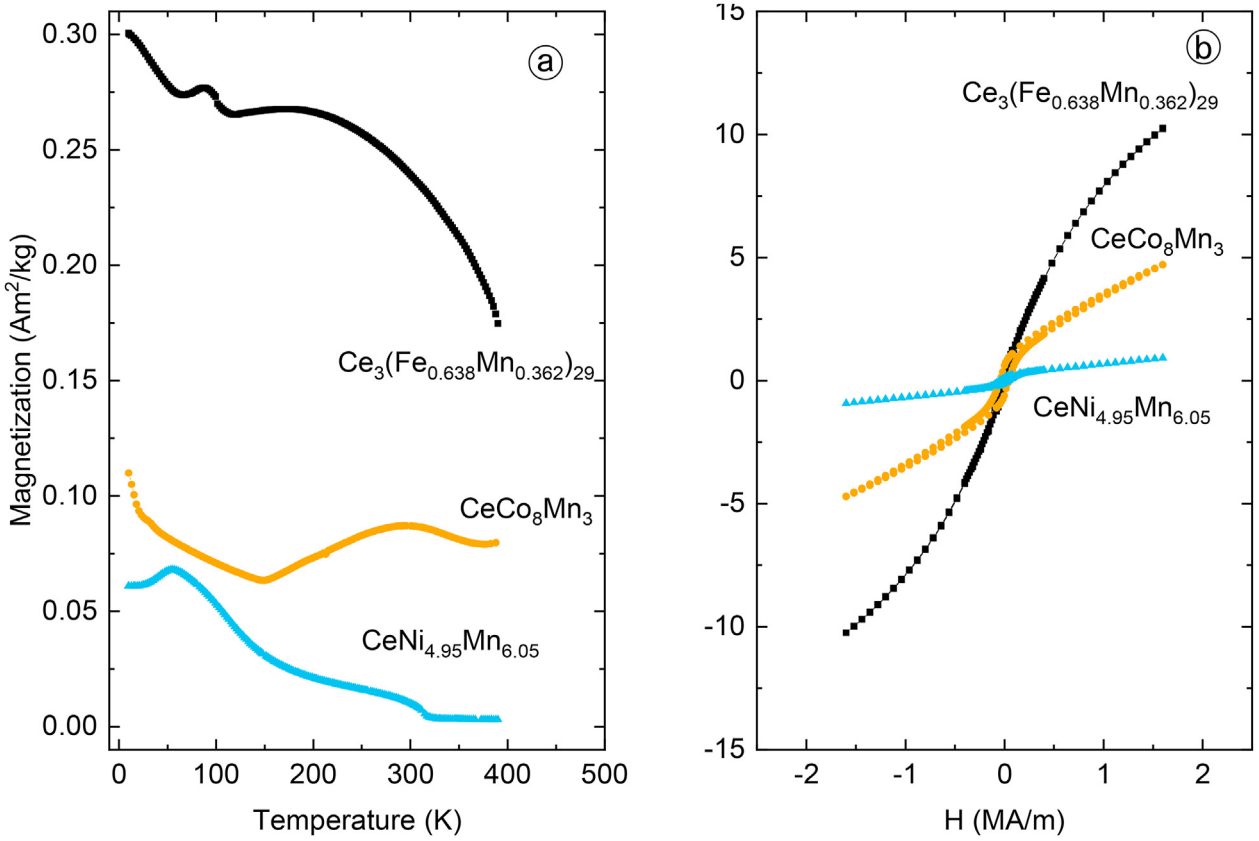

Fig. 4. (a) Magnetization versus temperature of $Ce_3(Fe_{0.638}Mn_{0.362})_{29}$, $CeCo_8Mn_3$ and $CeNi_{4.95}Mn_{6.05}$ in an applied magnetic field of 8 kA/m, $Ce_3(Fe_{0.638}Mn_{0.362})_{29}$ suggests ferrimagnetic ordering, while $CeNi_{4.95}Mn_{6.05}$ and $CeCo_8Mn_3$ indicates a canted antiferromagnetic state; (b) Magnetization versus applied field at 10 K for $Ce_3(Fe_{0.638}Mn_{0.362})_{29}$, $CeCo_8Mn_3$ and $CeNi_{4.95}Mn_{6.05}$.

54 K, which tentatively is attributed to a change in spin ordering and magnetic anisotropy. The canted antiferromagnetic state is supported by the results shown in Fig. 4(b); the magnetization at 10 K does not even reach 0.1 μ_B/f.u. (1 Am^2/kg) in an applied field of 1.6 MA/m. It should be noted that magnetic structures are best determined from neutron scattering or techniques capable of probing the atomic magnetic moments locally, such as muon spin spectroscopy or nuclear magnetic resonance. We give indicative descriptions of which magnetic ordering can be suggested for the new compounds described in this work, however, the previously mentioned techniques are needed to get more reliable information. The only published data for Ce in 1:11 was prepared by Manfretti et al. [15] where they found no evidence for a bulk magnetic ordering in $CeMn_{2.25}Cu_{8.75}$. We also display selected low field hysteresis curves in Fig. 5(a) at various temperatures of interest and for all three new compounds the extracted data can be found in Table 3. The comparably strong increase of the magnetic coercivity below the cusp temperature supports an explanation in terms of an increase in magnetic anisotropy below the cusp temperature.

Regarding the new $CeCo_8Mn_3$ and $Ce_3(Fe_{0.638}Mn_{0.362})_{29}$, the situation is more interesting. The low field magnetization versus temperature result of $CeCo_8Mn_3$, shown in Fig. 4(a), indicates a complex behavior with no clear indication of a magnetic ordering temperature. However, the magnetization versus field result shown in Fig. 4(b) again indicates a canted antiferromagnetic behavior. The canted antiferromagnetic state is supported by the fact that the magnetization only reaches about 0.6 μ_B/f.u. (5 Am^2/kg) in an applied field of 1.6 MA/m at 10 K. Moreover, a weak hysteretic behavior is observed at low fields, followed by an approximately linear field dependence at higher fields. Selected hysteresis curves recorded at different temperature are presented in Fig. 5(b), show that the characteristic low field hysteretic behavior of a canted antiferromagnetic state remains up at the highest temperature measured. Thus, the results indicate a magnetic ordering temperature for the canted antiferromagnetic state higher than 400 K.

The $Ce_3(Fe_{0.638}Mn_{0.362})_{29}$ compound exhibits a magnetic ordering temperature well above 400 K (the highest measuring temperature) and the hysteresis curve recorded at 10 K suggests a ferrimagnetic behavior, with a magnetization in applied fields of 1.6 MA/m and 4.8 MA/m reaching values of 3.7 and 16 μ_B/f.u. (10 and 43 Am^2/kg), respectively. The anomaly in the magnetization versus temperature curve for this compound at approximately 87 K, could be related to the 1.7 wt % impurity of CeO_2 observed for this sample. It should be noted that even binary Ce_2Fe_{17} exhibits a complicated magnetic behavior [30], and trying to unravel the origin behind features seen in the low field magnetization versus temperature result is beyond the scope of this work.

A summary of the suggested magnetic ordering with ordering temperature and magnetic moment can be found in Table 3. Together with the peculiarities in the crystallographic features of Ce together with transition metals, we expect that there are many other systems which require updates and revisiting of the data.

When studying new systems, whether it is for exploring heavy fermion systems such as $CeCu_6$ [31] or permanent magnets it is worth to note that some of these systems have extremely narrow homogeneity ranges and could possibly contain crystallographic phases from the same crystal family studied here. This will be of particular importance if any Ce based magnets are to be developed,

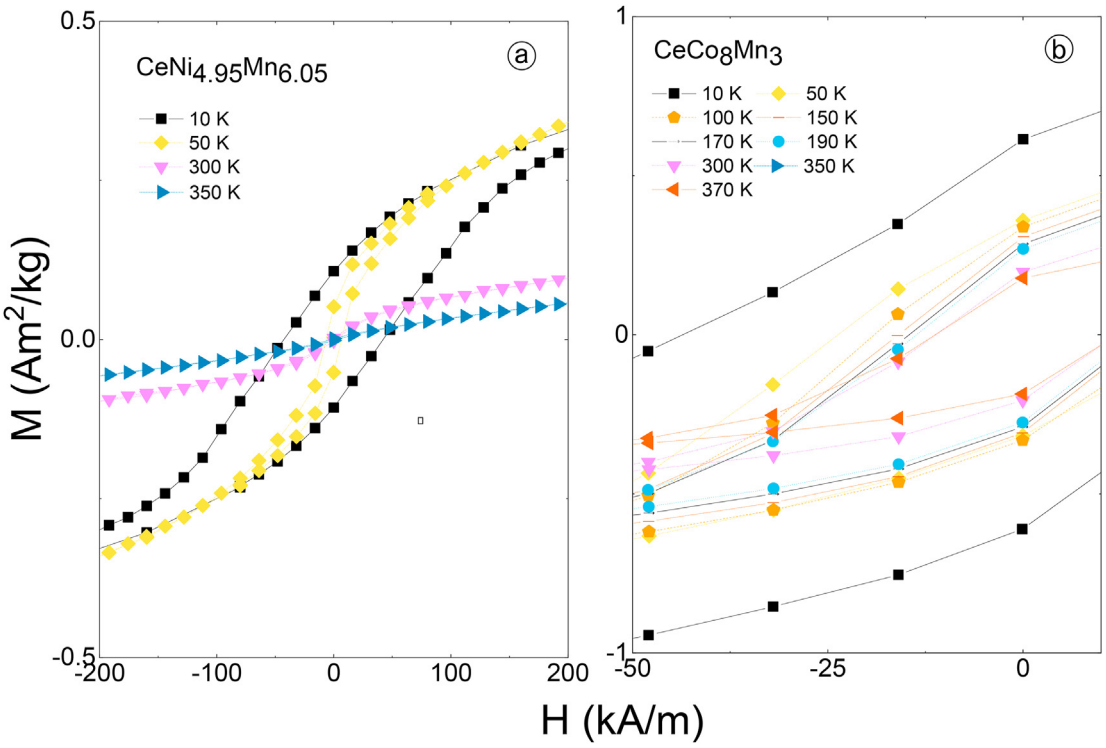

Fig. 5. Magnetization versus applied field for: (a) $CeNi_{4.95}Mn_{6.05}$ and (b) $CeCo_8Mn_3$ at different temperatures. The symbols and lines are shared between (a) and (b) and the interpretation of these can be seen in (b).

Table 3
Magnetization at an applied field of 1.6 MA/m at 10 K in units of Am^2/kg and μ_B/f.u together with the suggested magnetic ordering and ordering temperature.

Compound	M (10 K) (Am^2/kg)	M (10 K) (μ_B/f.u)	Suggested ordering	T_C or T_N (K)
$CeCo_8Mn_3$	5	0.6	Canted antiferromagnet	>400
$Ce_3(Fe_{0.638}Mn_{0.362})_{29}$	10	3.7	Ferrimagnet	>400
$CeNi_{4.95}Mn_{6.05}$	0.1	1	Canted antiferromagnet	300

as they will likely need extra elements to develop not only its intrinsic properties, but also the correct microstructure. In the prototypical $Nd_2Fe_{14}B$ magnets, additives of Al, Co, Cu, Dy, Ga, O and Tb are frequently present, not only to modify the intrinsic properties, but also to modify the microstructure.

4. Conclusion

In this study, it is shown that the Ce–Fe–Mn and Ce–Co–Mn phase diagrams need to be revised. It was found that new 3:29 and 1:11 compounds exist with different structures, compared to the 2:17. It is difficult to distinguish whether the compounds $Ce_3(Fe_{0.638}Mn_{0.362})_{29}$ and $CeCo_8Mn_3$ have excesses of Ce (could be presented as: $Ce_{3+x}(Fe,Mn)_{29}$ and $Ce_{1+x}(Co,Mn)_{11}$ respectively) or an extended homogeneity range, and whether these structures are ordered or disordered. Complex experimental datasets have been used to support our claim (XRD, SEM/EDS and SQUID magnetometry). Additionally, neutrons and Mössbauer results from literature for related compounds were taken into account. The interpretation of our results is supported by an extensive literature study on other *R–T–T'* systems. We also emphasize that the differences in homogeneity regions of the 1:11, 1:12, 2:17 and 3:29-phases are extremely subtle.

Thus, it is of utmost importance to use a multitude of characterization techniques when finding new systems to explore for new physical properties such as ferromagnetism. This could likely extend to other physical properties, such as the well-known Kondo materials like $CeCu_6$. For the samples investigated here results have been obtained indicating that $CeNi_{4.95}Mn_{6.05}$ and $CeCo_8Mn_3$ exhibit properties characteristic of canted antiferromagnetic states, while $Ce_3(Fe_{0.638}Mn_{0.362})_{29}$ orders ferrimagnetically with an ordering temperature well above room temperature.

CRediT authorship contribution statement

Vitalii Shtender: Investigation, Formal analysis, Writing - original draft. **Daniel Hedlund:** Conceptualization, Investigation, Formal analysis, Writing - original draft. **Simon Rosenqvist Larsen:** Investigation, Writing - review & editing. **Peter Svedlindh:** Methodology, Writing - review & editing. **Martin Sahlberg:** Methodology, Writing - review & editing.

Declaration of competing interest

The authors declare that they have no known competing financial interests or personal relationships that could influence the work reported in this paper.

Acknowledgement

This work was supported by the Swedish Foundation for Strategic Research, project "SSF Magnetic materials for green energy technology" (EM16-0039) who are gratefully acknowledged. This work was funded through SweGRIDS, by the Swedish Energy

Agency and Höganäs AB.

Appendix A. Supplementary data

Supplementary data to this article can be found online at https://doi.org/10.1016/j.jallcom.2020.157435.

References

[1] J.M.D. Coey, Perspective and Prospects for Rare Earth Permanent Magnets, Engineering, 2019, https://doi.org/10.1016/j.eng.2018.11.034.

[2] S. Dong, W. Li, H. Chen, R. Han, The status of Chinese permanent magnet industry and R&D activities, AIP Adv. 7 (2017), 056237, https://doi.org/10.1063/1.4978699.

[3] D.B. De Mooij, K.H.J. Buschow, Some novel ternary $ThMn_{12}$-type compounds, J. Less Common Met. 136 (1988) 207–215, https://doi.org/10.1016/0022-5088(88)90424-9.

[4] G.C. Hadjipanayis, A search for new Fe-rich phases for the development of permanent magnets, in: Concert. Eur. Action Magnets, Springer Netherlands, 1989, pp. 122–129, https://doi.org/10.1007/978-94-009-1135-2_9.

[5] A.M. Gabay, G.C. Hadjipanayis, Recent developments in RFe_{12}-type compounds for permanent magnets, Scripta Mater. 154 (2018) 284–288, https://doi.org/10.1016/j.scriptamat.2017.10.033.

[6] G.C. Hadjipanayis, A.M. Gabay, A.M. Schönhöbel, A. Martín-Cid, J.M. Barandiaran, D. Niarchos, $ThMn_{12}$-Type Alloys for Permanent Magnets, Engineering, 2019, https://doi.org/10.1016/j.eng.2018.12.011.

[7] Y.M. Kalychak, O.I. Bodak, E.I. Gladyshevskii, The ternary system Cerium-Manganese-Iron, Visn. Lviv. Derzh. Univ., Ser. Khim. 16 (1974) 11–15.

[8] I. Fartushna, A. Khvan, A. Dinsdale, V. Cheverikin, D. Ivanov, A. Kondratiev, An experimental investigation of liquidus and solidus projections for the Fe-Mn-Ce system, J. Alloys Compd. 654 (2016) 424–434, https://doi.org/10.1016/j.jallcom.2015.09.123.

[9] Y.M. Kalychak, O.I. Bodak, E.I. Gladyshevskij, Compounds of the $ThMn_{12}$ type in the systems Ce-Mn-[Fe, Co, Ni], Kristallografiya 21 (1976) 507–510.

[10] I. Fartushna, A. Khvan, A. Dinsdale, V. Cheverikin, D. Ivanov, A. Kondratiev, Phase equilibria in the Fe-Mn-Ce system at 900 °C, J. Alloys Compd. 658 (2016) 331–336, https://doi.org/10.1016/j.jallcom.2015.10.215.

[11] O.I. Bodak, Y.M. Kalychak, V.P. Skvorchuk, The Ce-Mn-Co system, Dopov. Akad. Nauk Ukr. RSR, Ser. A. 10 (1981) 82–86.

[12] Y.M. Kalychak, O.I. Bodak, E.I. Gladyshevskii, The system Ce-Mn-Ni, Inorg. Mater. 12 (1976) 961–965.

[13] Y.M. Kalychak, O.I. Bodak, G.B. Krasovskaya, Ce-Mn-Cu system, Dopov. Akad. Nauk Ukr. RSR, Ser. A. (1979) 867–869, n.d.

[14] J. Rodriguez-Carvajal, Recent developments in the program FullProf, in commission on powder diffraction (IUCr), Newsletter 26 (2001) 12–19.

[15] P. Manfrinetti, M.L. Fornasini, D. Mazzone, S.K. Dhar, R. Kulkarni, Crystal structure and magnetic properties of Cu-rich Ce-Mn-Cu intermetallics, J. Alloys Compd. 379 (2004) 64–71, https://doi.org/10.1016/j.jallcom.2004.03.072.

[16] A. Kuchin, A. Pirogov, V. Khrabrov, A. Teplykh, A. Ermolenko, E. Belozerov, Magnetic and structural properties of $Ce_2Fe_{17-x}Mn_x$ compounds, J. Alloys Compd. 313 (2000) 7–12, https://doi.org/10.1016/S0925-8388(00)01039-2.

[17] P. Villars, K. Cenzual, Pearson's Crystal Data – Crystal Structure Database for Inorganic Compounds, Release, ASM International, Materials Park, Ohio, USA, 2016/17 n.d.

[18] Z. Hu, W.B. Yelon, Structural and magnetic properties of the novel $Nd_3Fe_{29-x}Ti_x$ compound from powder neutron diffraction, Solid State Commun. 91 (1994) 223–226, https://doi.org/10.1016/0038-1098(94)90228-3.

[19] C.D. Fuerst, F.E. Pinkerton, J.F. Herbst, On the Formation of $NdFe_{9.5-x}T_x$ compounds (T = Ti, Cr, Mn), J. Chem. Inf. Model. 129 (1994), https://doi.org/10.1017/CBO9781107415324.004. L115–L119.

[20] C.D. Fuerst, F.E. Pinkerton, J.F. Herbst, Structural and magnetic properties of $R_3(Fe,T)_{29}$ compounds, J. Appl. Phys. 76 (1994) 6144–6146, https://doi.org/10.1063/1.358334.

[21] H.L. Liu, M. Huang, Q. Feng, The Mössbauer spectrum Research of the lanthanon compound $Tb_3Fe_{29-x}Cr_x$, Mater. Sci. Forum 650 (2010) 347–354. https://doi.org/10.4028/www.scientific.net/MSF.650.347.

[22] W.B. Pearson, The Crystal Chemistry and Physics of Metals and Alloys, Wiley-Interscience, New York, 1972.

[23] O.I. Bodak, D.O. Berezyuk, L.V. Gavriliv, Kotur, The ternary system Ce-Fe-Cr, Visn. Lviv. Derzh. Univ., Ser. Khim. 33 (1994) 5–7.

[24] Z.G. Sun, S.Y. Zhang, H.W. Zhang, J.Y. Wang, B.G. Shen, The effect of manganese substitution on the magnetic properties of Ce_2Co_{17} compounds, J. Phys. Condens. Matter 12 (2000) 2495–2504, https://doi.org/10.1088/0953-8984/12/11/315.

[25] A. Popescu, O. Isnard, R. Dudric, M. Coldea, X-ray photoelectron spectroscopy and magnetic properties of $Ce_2Co_{15}Mn_3$ compound, J. Alloys Compd. 535 (2012) 10–14, https://doi.org/10.1016/j.jallcom.2012.04.047.

[26] W. Wang, J. Wang, W. Li, B. Liu, G. Wu, H. Jin, F. Yang, Structural and magnetic properties of $Sm_3(Fe_{1-x}Co_x)_{29-y}Cr_y$ compounds, J. Alloys Compd. 358 (2003) 12–16, https://doi.org/10.1016/S0925-8388(03)00065-3.

[27] O. Kalogirou, V. Psycharis, L. Saettas, D. Niarchos, Existence range, structural and magnetic properties of $Nd_3Fe_{27.5}Ti_{1.5-y}Mo_y$ and $Nd_3Fe_{27.5}Ti_{1.5-y}Mo_yN_x$ ($0.0 \leq y \leq 1.5$), J. Magn. Magn Mater. 146 (1995) 335–345, https://doi.org/10.1016/0304-8853(94)01694-1.

[28] Q. Johnson, D.H. Wood, G.S. Smith, The crystal structure of Pu_3Zn_{22}, Acta Crystallogr. Sect. B Struct. Crystallogr. Cryst. Chem. 24 (1968) 480–484, https://doi.org/10.1107/S0567740868002682.

[29] X.-F. Han, F.-M. Yang, Q.-S. Li, M.-C. Zhang, S.-Z. Zhou, Crystallographic and magnetic properties of $R_3Fe_{29-x}V_xN_4$ (R = Y, Ce, Nd, Sm, Gd, Tb, and Dy), J. Phys. Condens. Matter 10 (1998) 151–163, https://doi.org/10.1088/0953-8984/10/1/017.

[30] O. Prokhnenko, C. Ritter, Z. Arnold, O. Isnard, J. Kamarád, A. Pirogov, A. Teplykh, A. Kuchin, Neutron diffraction studies of the magnetic phase transitions in Ce_2Fe_{17} compound under pressure, J. Appl. Phys. 92 (2002) 385–391, https://doi.org/10.1063/1.1485111.

[31] Y. Ōnuki, Y. Shimizu, T. Komatsubara, Magnetic property of a new Kondo lattice intermetallic compound: $CeCu_6$, J. Phys. Soc. Jpn. 53 (1984) 1210–1213, https://doi.org/10.1143/JPSJ.53.1210.